ISSN 0021-3640, JETP Letters, 2013, Vol. 98, No. 1, pp. 19–23. © Pleiades Publishing, Ltd., 2013.
Original Russian Text © S.N. Martynov, 2013, published in Pis'ma v Zhurnal Eksperimental'noi i Teoreticheskoi Fiziki, 2013, Vol. 98, No. 1, pp. 23–27.

Incommensurate Magnetic Structures in Rhombohedral Heisenberg Antiferromagnet

S. N. Martynov

Kirensky Institute of Physics, Siberian Branch, Russian Academy of Sciences, Krasnoyarsk, 660036 Russia

e-mail: unonav@iph.krasn.ru

Received April 23, 2013; in final form, May 27, 2013

The phase diagram of the ground state has been calculated for a rhombohedral antiferromagnet of the *R*3*m* symmetry with frustrated exchange in the base plane and competition of exchanges between the nearest and next-nearest planes. The diagram contains phases of collinear antiferromagnetic ordering of various types separated by five incommensurate magnetic states of the helicoidal type, differing in the ordering type and in the direction of the modulation vector. The commensurate and incommensurate phases converge at multicritical points lying on a line corresponding to an antiferromagnet with an undistorted simple cubic lattice.

DOI: 10.1134/S0021364013140099

Increased interest in incommensurate magnetic structures in the last decade has primarily been stimulated by the discovery of multiferroic properties in many of them [1]. The helical ordering of spins is accompanied by the disappearance of the center of symmetry and is responsible for the appearance of electric polarization. The local polarization $\mathbf{p}_{ij}$ in many mechanisms of the ferroelectric effect [2–4] is attributed to the noncollinearity of spins. In particular, for the model with the inverse effect of the Dzyaloshinskii–Moriya interaction [4],

$$\mathbf{p}_{ij} \propto \mathbf{e}_{ij} \times (\mathbf{S}_i \times \mathbf{S}_j), \quad (1)$$

where $\mathbf{e}_{ij}$ is the unit vector connecting the spins. As a result, both the direction of the spontaneous polarization and the magnetoelectric effect (dependence of the polarization on the applied magnetic field) are determined by the orientation of the modulation and polarization vectors of incommensurate magnetic structures. In describing incommensurate magnetic structures with large modulation vectors, when the angles between the interacting spins are comparable to 90°, the competition (frustration) between symmetric exchanges is treated as the primary mechanism of the formation of the structure. The antiferromagnetic Dzyaloshinskii–Moriya exchange for ions of a transition group is relatively small and leads to the formation of long-period structures [5]. For quasi-one-dimensional magnetic structures with the competition of exchanges between the nearest (J_{nn}) and next-nearest (J_{nnn}) magnetic neighbors in the chain, e.g., $LiCu_2O_2$ [6], $LiCuVO_4$ [7], $CuCl_2$ [8], and $CuBr_2$ [9], the modulation vector is directed along the chain. In these multiferroics, $J_{nnn} \geq J_{nn}$, which leads to a large noncollinearity of spins. In the CuO multiferroic with the maximum temperature of the appearance of magnetically induced electric polarization, the ground state is quasidegenerate in the orientation of the magnetic moments in neighboring planes owing to a large number of competing exchanges [10, 11]. As a result, the transition to the long-period helicoidal phase with the modulation-vector direction intermediate with respect to crystal axes is accompanied by the rotation of the moments in the neighboring planes at an angle close to 90° (transition from the antiferromagnetic ordering AF1 to the modulated phase AF2 [10]). This rotation makes the main contribution to the electric polarization. In hexagonal and rhombohedral magnets, the geometrical frustration of the antiferromagnetic exchange in the planes with a triangular lattice of vector spins initiates the 120° orientation of magnetic moments. The appearance of incommensurate magnetic structures in a number of such systems is also accompanied by the appearance of the electric polarization [4, 12, 13]. Taking into account the direct dependence of the polarization on the noncollinearity of magnetic moments (1), such geometrically frustrated magnets are considered as promising candidates for multiferroics with strong magnetoelectric coupling [12]. The problem of allowed incommensurate magnetic structures in three-dimensional frustrated magnets with such symmetry has not yet been analyzed. The aim of this work is to determine the form and conditions of the appearance of incommensurate magnetic structures in a rhombohedral antiferromagnet of the R3m symmetry with the geometrical frustration of the exchange between nearest magnetic neighbors in the basal plane and competition of exchange interactions between the nearest and next-nearest planes.

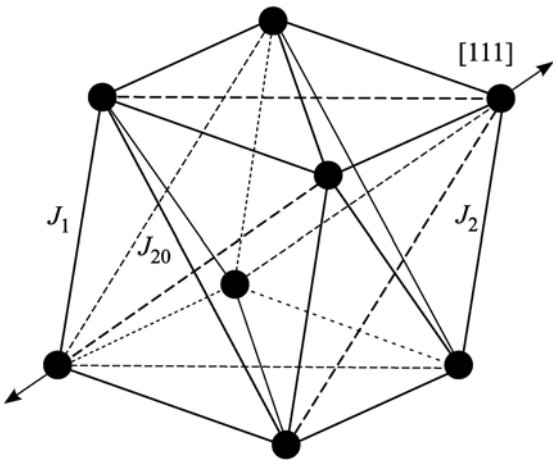

Fig. 1. Exchange interactions in the unit cell of a rhombohedral crystal.

The Hamiltonian of the model has the form

$$H = J_1\sum_{ij}\mathbf{S}_i\mathbf{S}_j + J_2\sum_{ij'}\mathbf{S}_i\mathbf{S}_{j'} + J_{20}\sum_{ij''}\mathbf{S}_i\mathbf{S}_{j''}, \qquad (2)$$

where J_1 and J_2 are the exchanges between the nearest and next-nearest planes, respectively, and J_{20} is the exchange between spins in the basal (111) plane (Fig. 1).

In the absence of rhombohedral distortion in the simple cubic lattice ($J_2 = J_{20}$), there are two types of collinear ordering depending on the relation between the J_1 and J_2 antiferromagnetic exchanges [14]. The first type (AF1) is the planes of spins with the parallel orientation that are orthogonal to the diagonals of the cube. An antiferromagnetic order is established between neighboring planes. Such a structure has the minimum energy in the J_1 exchange and is completely frustrated in the J_2 exchange. The second type of ordering (AF2) is the planes of antiferromagnetically ordered spins repeating along one of the axes of the crystal (a, b, or c). Such a structure is partially frustrated in both exchanges. Rhombohedral distortion (along the [111] diagonal in Fig. 1) holds both types of antiferromagnetic ordering, changing the exchange energy. The energy of one spin in the ground state for the AF1 and AF2 phases divided by $J_{20}S^2$ has the form

$$\begin{aligned}\epsilon_1 &= 3 - 3j_1 + 3j_2,\\ \epsilon_2 &= -1 - j_1 - j_2,\end{aligned} \qquad (3)$$

where $j_1 = J_1/J_{20}$ and $j_2 = J_2/J_{20}$. The boundary between the AF1 and AF2 phases on the (j_1j_2) phase plane is the straight line

$$j_2 = 0.5j_1 - 1. \qquad (4)$$

The incommensurate magnetic structure in the three-dimensional lattice constitutes the planes of collinearly (ferro- or antiferromagnetically) oriented spins whose orientations in the neighboring planes differ from each other by constant angle φ. The case of noncollinear orientation of spins in initial planes will be considered below. The necessary condition of the existence of such a structure is the presence of the frustrated (positive) exchange energy of interactions with planes following the nearest plane: second (ϵ_{2n}), third (ϵ_{3n}), etc., in the initial commensurate configuration of spins. In a rhombohedrally distorted cubic lattice (Fig. 1), there are ten variants of the choice of initial planes of spins with the energy $\epsilon_{2n} \neq 0$. Variants with initial planes interacting with more remote planes do not give incommensurate states. Depending on the type of ordering of spins in the initial planes and, therefore, the energy of exchange bonds inside the initial plane (ϵ_0) and between planes (ϵ_{1n} and ϵ_{2n}), different incommensurate magnetic structures appear at different relations between exchanges (2). The AF1 ordering is symmetric with respect to the rhombohedral axis. The operations of symmetry join the initial planes into four subgroups invariant with respect to the energies of exchange interactions ϵ_0, ϵ_{1n}, and ϵ_{2n}: $(111)_1$, $\{11\bar{1}\}_1$, $\{110\}_1$, and $\{1\bar{1}0\}_1$. Here and below, the planes are denoted in the rhombohedral basis. The subscript indicates the type of magnetic ordering in the plane. The remaining planes in the last three subgroups are obtained by the permutation of indices. The AF2 collinear ordering reduces symmetry, separating one of the directions in the crystal (a, b, or c). As a result, ten planes of the single-domain crystal where the antiferromagnetic plane is repeated along the c axis are joined into seven subgroups: $(111)_2$, $\{1\bar{1}1\}'_2$, $\{11\bar{1}\}_2$, $\{110\}_2$, $\{(1\bar{1}0)\}_2$, $\{101\}'_2$, and $\{10\bar{1}\}'_2$. The prime in the notation of the subgroups means the permutation of only the first two indices. Since the collinear ordering of the first type is completely frustrated in the exchanges with the next-nearest neighbors, J_2 and J_{20}, all planes with such a type of ordering have frustrated exchanges with the next-nearest planes ($\epsilon_{2n} > 0$). Among the planes with the second type of ordering, this necessary condition is satisfied only for the $(11\bar{1})_2$, $(110)_2$, and $(1\bar{1}0)_2$ planes. The energy of each spin in the helicoidal phase has the form

$$\epsilon = \epsilon_0 + \epsilon_{1n}\cos\varphi + \epsilon_{2n}\cos 2\varphi. \qquad (5)$$

The solution with $\varphi = 0$ gives the energies of the AF1 and AF2 phases (3):

$$\epsilon = \epsilon_0 + \epsilon_{1n} + \epsilon_{2n} = \epsilon_{1,2}. \qquad (6)$$

The minimization of the energy in the angle of helicoid φ provides the equilibrium value of cosφ and the threshold condition for the energies ϵ_{1n} and ϵ_{2n} under which the helicoidal solution exists:

$$\cos\varphi = -\epsilon_{1n}/4\epsilon_{2n}, \quad 4\epsilon_{2n} > |\epsilon_{1n}|. \qquad (7)$$

Under the threshold condition, the energy per spin of the helicoid is given by the expression

$$\epsilon = \epsilon_0 - \epsilon_{2n} - \epsilon_{1n}^2/8\epsilon_{2n}. \quad (8)$$

Incommensurate magnetic structures with the initial planes $\{11\bar{1}\}_1$ and $\{110\}_1$ have energies higher than those of remaining commensurate and incommensurate structures at any antiferromagnetic exchanges (2). The remaining five incommensurate magnetic structures are the ground states in various regions of the $(j_1 j_2)$ phase plane. The threshold conditions, $\cos\varphi$ values, and the energies of helicoidal states with the initial planes $(klm)_{1,2}$ have the form

$$\begin{aligned}
&(111)_1: \quad j_2 > j_1/4, \quad \cos\varphi = -j_1/4j_2,\\
&\epsilon = \epsilon_1 - 3(4j_2 - j_1)^2/8j_2;\\
&\{1\bar{1}0\}_1: \quad j_2 > j_1 - 3, \quad \cos\varphi = (j_1 - j_2 - 1)/2,\\
&\epsilon = \epsilon_1 - (3 + j_2 - j_1)^2/2;\\
&\{11\bar{1}\}_2: \quad j_2 > 2 + j_1/4, \quad \cos\varphi = j_1/4(j_2 - 2),\\
&\epsilon = \epsilon_2 - (4j_2 - j_1 - 8)^2/8(j_2 - 2);\\
&(110)_2: \quad j_2 > j_1 + 1, \quad \cos\varphi = -(j_1 + j_2 + 1)/2j_2,\\
&\epsilon = \epsilon_2 - (j_1 - j_2 + 1)^2/2j_2;\\
&(1\bar{1}0)_2: \quad j_2 < 1 - j_1, \quad \cos\varphi = -(j_1 + j_2 + 1)/2,\\
&\epsilon = \epsilon_2 - (j_1 + j_2 - 1)^2/2,
\end{aligned} \quad (9)$$

where ϵ_1 and ϵ_2 are the energies of the collinear phases given by Eqs. (3). The spins in the $(111)_1$, $(110)_2$, and $(1\bar{1}0)_2$ planes are oriented ferromagnetically and the spins in the $(1\bar{1}0)_1$ and $(11\bar{1})_2$ planes are oriented antiferromagnetically.

The boundaries between the commensurate and incommensurate phases on the phase plane are determined from the equality of the energies given by Eqs. (3) and (9). The phase diagram (Fig. 2) consists of the straight lines of second-order phase transitions in which incommensurate magnetic structures with $\varphi \longrightarrow 0$ appear and curves of first-order phase transitions, where a incommensurate magnetic structure appears with a finite value $\varphi > 0$. In this case, the type of ordering in planes changes. Both the length of the modulation vector (φ value) and its direction change at the boundaries between different helicoidal phases. Two commensurate and two incommensurate phases converge at the multicritical point $(j_1 = 4, j_2 = 1)$. At this point, the lines of the threshold conditions on the appearance of all incommensurate phases with the first type of ordering in the initial $(klm)_1$ planes converge, including those with a high energy. The lines of the threshold conditions for $(klm)_2$ helicoids converge

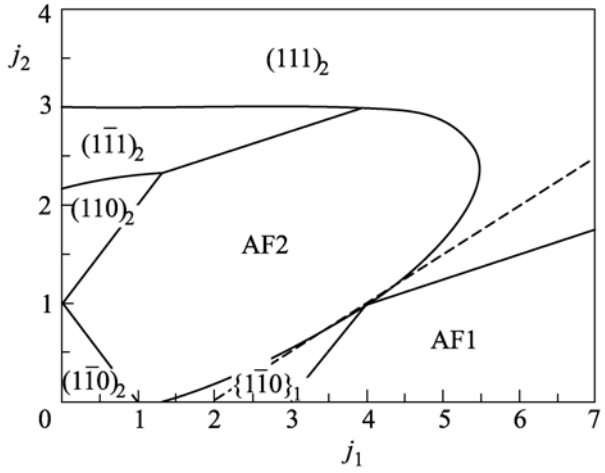

Fig. 2. Phase diagram of the magnetic states of a rhombohedral crystal. The dashed line is the boundary between the AF1 and AF2 collinear phases disregarding the effect of helicoidal phases $(klm)_{1,2}$ (4).

at the second multicritical point $(j_1 = 0, j_2 = 1)$. The indicated points are located on the straight line $j_2 = 1$, which corresponds to the undistorted cubic lattice and is the only straight line on the phase plane that does not include incommensurate phases. At the coordinate origin, $j_1 = j_2 = 0$, the $(1\bar{1}0)_2$ incommensurate phase is continuously confirmed to the 120° ordering of spins in a triangular rhombohedral plane. The resulting phase diagram is simply generalized to the case of the ferromagnetic exchange between neighboring basal (111) planes $(J_1 < 0)$ through the reflection with respect to the j_2 axis (Fig. 2). In this case, ordering in the planes changes from ABCABC to A(−B)C(−A)B(−C), where the minus sign means a change in the direction of all spins to the opposite direction in a given plane at each type of ordering. The AF2 type of collinear ordering is transferred to the third AF3 type of the collinear antiferromagnetic ordering and the AF1 ordering is transferred to the ferromagnetic ordering of all spins. In this case, the third multicritical point $(j_1 = -4, j_2 = 1)$ appears. The generalization to the case with ferromagnetic exchange $J_2 < 0$ is not so trivial and requires individual analysis.

In crystals where the number of magnetic neighbors in each type of antiferromagnetic exchange is multiple of three, four-sublattice noncollinear ordering can exist, as in geometrically frustrated antiferromagnets with a pyrochlore lattice [15] (Fig. 3). If additional anisotropic interactions are disregarded, such a ground state is continuously degenerate in the angles Θ and ϕ; as a result, the long-range magnetic order is absent at zero temperature. The rhombohedral lattice of spins can also exhibit four-sublattice ordering at which the spins of each sublattice interact only with the spins of the other three sublattices in all three types of exchanges (2) (Fig. 4). The energy of this ordering

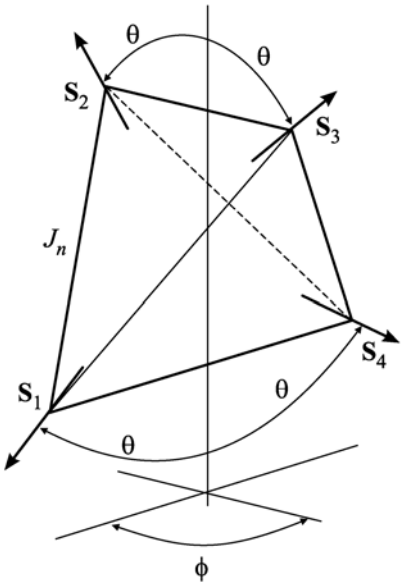

Fig. 3. Orientation of the spins at four-sublattice ordering.

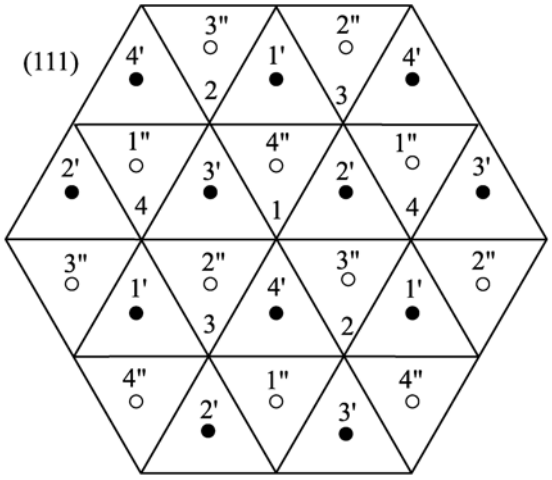

Fig. 4. Projection of four magnetic sublattices on the basal (111) plane. The spins of each sublattice of the basal plane interact only with spins of other sublattices both in the plane (solid lines) and between nearest (closed circles) and next-nearest (open circles) planes.

is ϵ_2. At the coplanar orientation of the spins of the sublattices ($\phi = 0$), helicoidal ordering with the conservation of total coplanarity is possible. However, threshold conditions are enhanced in this case as compared to collinear ordering of the second type (AF2) in planes. For incommensurate magnetic structures with the initial $(11\bar{1})$ plane, we obtain

$$(j_2 - 1)\cos(2\Theta) > 1 + j_1/4. \quad (10)$$

For the same exchanges, the energy of the helicoid with $(11\bar{1})_2$ is always lower than the energy of the helicoid with $\Theta > 0$. Threshold conditions and energies for incommensurate magnetic structures with other initial planes also change. This means that the energy of excited states with collinear ordering in region AF2 (see Fig. 2), where helicoids are not ground states, is also lower than the excitation energies of noncollinear states. Therefore, the free energy of collinear ordering at finite temperature is lower than the energy of noncollinear states; for this reason, ordering occurs through disorder [15, 16]. Continuous degeneracy is lifted by incommensurate states both outside and inside region AF2 (see Fig. 2).

In the absence of the inversion center, the antisymmetric Dzyaloshinskii–Moriya exchange $\sum_{ijn} \mathbf{D}_n (\mathbf{S}_i \times \mathbf{S}_j)$, where n is the index of the corresponding exchange bonds in Eq. (2), between interacting spins appears as an additional mechanism of spin noncollinearity. It can lead either to weak ferromagnetism [17] or to incommensurate magnetic structure [18], lifting degeneracy of the AF2 phase [19]. In the former case, the AF1 and AF2 phases become weak ferromagnetic, whereas helicoidal states (9) become modulated (double) helicoids, as incommensurate magnetic structures of the high-temperature phase in CuB_2O_4 [20]. In the latter case, the incommensurate modulation of the AF1 and AF2 phases depends on the distribution of the directions of Dzyaloshinskii vectors $\mathbf{D}_n$ and their lengths. When the components $\mathbf{D}_1$ and $\mathbf{D}_2$ along the [111] direction dominate, incommensurate magnetic structures in these phases have the wave vector $\mathbf{k}$(kkk). The phase boundary between the AF1 and $(111)_1$ phases disappears because both phases have the same direction of the modulation vectors and the same type of magnetic order in the initial plane. The other phase boundaries hold because a transition through them is accompanied by a change either in the order parameter in planes or in the direction of the vector $\mathbf{k}$. The form of incommensurate magnetic structures is complicated, but the noncollinearity of neighboring interacting spins and, therefore, the polarization in ferroelectric (1) are determined by the strongest mechanism of incommensurability. For the ions of the transition group with the small contribution from the spin–orbit interaction, the change in the energy of commensurate and incommensurate phases is about D_n^2/J_n. Correspondingly, the change in the threshold conditions and boundaries between phases is of the same order of magnitude.

To summarize, the existence of five different helicoidal structures is a feature of this type of crystal lattice. Individual sets of incommensurate magnetic structures will exist in other frustrated lattices under the corresponding threshold relations for the exchange interactions. In particular, only a helicoid with the modulation vector along the tetragonal axis can appear in a body-centered tetragonal lattice with three

nearest exchanges [21]. However, the distortion of the rhombohedral crystal leading to the reduction of symmetry (e.g., to the monoclinic symmetry $C2/m$, as in delafossite $CuFeO_2$ [4, 22] with a decrease in the temperature) can result in a change in the number of allowed incommensurate magnetic structures only through a change in the corresponding exchanges and, as a result, threshold conditions. Consequently, the disappearance of incommensurate magnetic structures existing in the high-symmetry phase and the appearance of new phases in the low-symmetry phase (in the phase space with a higher dimension) are possible primarily near multicritical (including tricritical) points of the high-symmetry phase. The following topological rule can be formulated: the phase diagram of a partially frustrated Heisenberg magnet consists of commensurate phases, which are separated by incommensurate phases, and multicritical points lying on the line of the high-symmetry phase.

I am grateful to A.I. Pankrats for stimulating discussions.

REFERENCES

1. T. Kimura, T. Goto, H. Shintani, et al., Nature (London) **423**, 55 (2003); S.-W. Cheong and M. Mostovoy, Nature Mater. **6**, 13 (2007).
2. H. Katsura, N. Nagaosa, and A. V. Balatsky, Phys. Rev. Lett. **95**, 057205 (2005); M. Mostovoy, Phys. Rev. Lett. **96**, 067601 (2006); A. S. Moskvin, Yu. D. Panov, and S.-L. Drechsler, Phys. Rev. B **79**, 104112 (2009).
3. I. A. Sergienko and E. Diagotto, Phys. Rev. B **73**, 094434 (2006).
4. T. Arima, J. Phys. Soc. Jpn. **76**, 073702 (2007).
5. Yu. A. Izyumov, *Neutron Diffraction in Long Periodic Structures* (Energoatomizdat, Moscow, 1987) [in Russian].
6. T. Matsuda, A. Zheludev, B. Roessli, et al., Phys. Rev. B **72**, 014405 (2005); S. Park, Y. I. Choi, C. I. Zhang, and S. W. Cheong, Phys. Rev. Lett. **98**, 057601 (2007); Y. Naito, K. Sato, Y. Yasui, et al., J. Phys. Soc. Jpn. **76**, 023708 (2007).
7. H. J. Xiang and M.-H. Whangbo, Phys. Rev. Lett. **99**, 257203 (2007); Y. Yasui, Y. Naito, K. Sato, et al., J. Phys. Soc. Jpn. **77**, 023712 (2008).
8. M. G. Banks, R. K. Kremer, C. Hoch, et al., Phys. Rev. B **80**, 024404 (2009); S. Seki, T. Kurumaji, S. Ishiwata, et al., Phys. Rev. B **82**, 064424 (2010).
9. C. Lee, J. Liu, M.-H. Whanbo, et al., Phys. Rev. B **86**, 060407(R) (2012).
10. G. Giovanneti, S. Kumar, A. Stroppa, et al., Phys. Rev. Lett. **106**, 026401 (2011).
11. P. Babkevich, A. Poole, R. D. Johnson, et al., Phys. Rev. B **85**, 134428 (2012); G. Jin, K. Cao, G.-C. Guo, and L. He, Phys. Rev. Lett. **108**, 187205 (2012); R. Villareal, G. Quirion, M. L. Plumer, et al., Phys. Rev. Lett. **109**, 167206 (2012).
12. T. Kimura, J. C. Lashley, and A. P. Ramirez, Phys. Rev. B **73**, 220401(R) (2006).
13. R. D. Johnson, L. C. Chapon, D. D. Khalyavin, et al., Phys. Rev. Lett. **108**, 087201 (2012); N. Terada, D. D. Khalyavin, P. Manuel, et al., Phys. Rev. Lett. **109**, 097203 (2012).
14. D. ter Haar and M. E. Lines, Philos. Trans. R. Soc. London A **254** (1046), 521 (1962).
15. R. Moessner and J. T. Chalker, Phys. Rev. B **58**, 12049 (1998).
16. J. Villain, R. Bidaux, J. P. Canon, and R. J. Conte, J. Phys. (Paris) **41**, 1263 (1980); E. F. Shender, Sov. Phys. JETP **56**, 178 (1982); C. L. Henley, J. Appl. Phys. **61**, 3962 (1987).
17. I. Dzyaloshinsky, J. Phys. Chem. Solids **4**, 241 (1958); T. Moriya, Phys. Rev. **120**, 91 (1960).
18. I. E. Dzyaloshinskii, Sov. Phys. JETP **19**, 960 (1964).
19. M. Elhajal, B. Chanals, R. Sunyer, and C. Lacroix, Phys. Rev. B **71**, 094420 (2005).
20. S. N. Martynov, J. Exp. Theor. Phys. **109**, 979 (2009).
21. J. S. Smart, *Effective Field Theories of Magnetism* (Saunders, London, 1966; Mir, Moscow, 1968).
22. Y. Tanaka, N. Terada, T. Nakajima, et al., Phys. Rev. Lett. **109**, 127205 (2012).

Translated by R. Tyapaev